doi: 10.4149/gpb_2025033

2-*epi*-Jaspine B induces mitochondria-mediated and autophagic cell death *via* ceramide overload in a cervical cancer model

Alexandra Kešeľáková[1], Natália Nosálová[1], Monika Majirská[1], Martin Kello[1], Radka Michalková[1], Miroslava Martinková[2,3], Tatiana Pončáková[2,3] and Martina Bago Pilátová[1]

[1] *Department of Pharmacology, Faculty of Medicine, Pavol Jozef Šafárik University, Košice, Slovak Republic*
[2] *Institute of Chemical Sciences, Department of Organic Chemistry, Faculty of Science, Pavol Jozef Šafárik University, Košice, Slovak Republic*
[3] *Juhapharm, Ltd., Košice, Slovak Republic*

Abstract. Marine-derived sphingolipids exhibit diverse biological activities, including notable anticancer properties that have recently garnered increasing scientific interest. This study aimed to evaluate the antiproliferative activity of a newly synthesized compound, 2-*epi*-jaspine B hydrochloride (M1), a cyclic anhydrophytosphingosine derivative, in an *in vitro* model using human cervical carcinoma (HeLa) cells. The antiproliferative effect of M1 was assessed *via* the MTS metabolic assay, which yielded an IC_{50} value of 5.6 ± 0.32 μmol/l. Flow cytometry and Western blot analyses demonstrated that M1 effectively induced both intrinsic and extrinsic apoptotic pathways, along with autophagic cell death. These effects were mediated through modulation of sphingolipid metabolism, resulting in the accumulation of ceramide, a key pro-apoptotic lipid. Our findings highlight the multiple mechanisms of action of M1 and its significant potential as an anticancer agent. By targeting sphingolipid metabolic pathways, 2-*epi*-jaspine B not only impairs cell proliferation but also triggers programmed cell death through multiple pathways. These results support the potential of marine-derived sphingolipid analogs, such as M1, for future development as therapeutic agents in the treatment of cervical cancer and possibly other malignancies.

Key words: Sphingolipid — Apoptosis — Autophagy — Cancer — Ceramide

Highlights:

- 2-*epi*-jaspine B is a new analog of a marine natural product, jaspine B
- 2-*epi*-jaspine B inhibits the proliferation of cervical carcinoma cells
- 2-*epi*-jaspine B showed pro-apoptotic potential on HeLa cells
- 2-*epi*-jaspine B induced autophagic cell death
- 2-*epi*-jaspine B interferes with sphingolipid metabolism and increases ceramide levels
- 2-*epi*-jaspine B is a promising candidate for future anticancer drug development

Correspondence to: Martina Bago Pilátová, Department of Pharmacology, Faculty of Medicine, Pavol Jozef Šafárik University, 040 11 Košice, Slovak Republic
E-mail: martina.pilatova@upjs.sk

© The Authors 2026. This is an **open access** article under the terms of the Creative Commons Attribution-NonCommercial 4.0 International License (https://creativecommons.org/licenses/by-nc/4.0/), which permits non-commercial use, distribution, and reproduction in any medium, provided the original work is properly cited.

Introduction

Cervical cancer (CC), the fourth most common malignancy among women worldwide, represents a significant health challenge in gynecological oncology (Bray et al. 2024). In 2020, an estimated 4.4 million cancer-related deaths in women resulted in approximately 1,047,000 new maternal orphans globally, with cervical cancer accounting for 20% of these cases (Guida et al. 2022). Currently, standard treatment for CC includes chemotherapy (typically cisplatin) alongside local therapies such as radiotherapy and surgery to improve patient outcomes (Knoff et al. 2014). However, despite advancements in combination therapy, the prognosis for patients with metastatic CC remains poor due to a high risk of relapse, primarily driven by increasing resistance of tumor cells to chemotherapeutic agents (George et al. 2022). Moreover, these treatments are often associated with significant adverse effects that further limit their therapeutic efficacy (Nurgali et al. 2018). Therefore, the development of novel anticancer agents with greater effectiveness and fewer side effects is essential to enhance therapeutic success and mitigate the broader societal impact of cervical cancer.

Recent studies have shown the significant role of bioactive sphingolipids in cancer progression and resistance against chemo- and radiotherapy (Furuya et al. 2011). Sphingolipids are essential structural components of cellular membranes playing an important role in regulating fluidity and maintaining barrier function (Hannun and Obeid 2008). Ceramide (Cer), a central intermediate in sphingolipid metabolism, is formed by a fatty acid amido-linked to sphingosine (Sph) backbone (Ogretmen and Hannun 2004). It is generated by three independent pathways including the *de novo* synthesis, sphingomyelin (SM) hydrolysis by sphingomyelinases (SMases) and salvage pathway (Kitatani 2008). Cer and Sph are typically known to mediate antiproliferative responses such as induction of apoptosis, growth arrest, and/or endoplasmic reticulum (ER) stress, autophagy and senescence (Ogretmen 2018). However, the metabolic conversion of Cer to glycosylated or phosphorylated members of the sphingolipid family contributes to cellular survival and resistance (Adan-Gokbulut 2013). Sphingosine-1-phosphate (S1P), a product arising from the phosphorylation of sphingosine by sphingosine kinases, is considered to be a tumor-promoting lipid involved in cell growth, proliferation, angiogenesis, and vasculogenesis (Pyne and Pyne 2010). Elevated levels of S1P counteract the proapoptotic effect of Cer, therefore Cer/S1P ratio determines the cell fate (Newton et al. 2015). Current knowledge suggests that regulating the induction of apoptosis or cross talk of apoptosis and autophagy by ceramide-like analogues may be helpful in the development of novel anticancer agents (Alizadeh et al. 2023).

In recent years, natural products have emerged as an alternative to current chemotherapeutic drugs. According to literature reports, natural compounds have biological properties such as antibacterial, antioxidant and antitumor (Kumar and Adki 2018). Among them, various marine-based drugs have shown anticancer activity through the induction of apoptosis (Chaudhry et al. 2022). Jaspine B is a cyclic anhydrophytosphingosine isolated from a marine sponge, *Pachastrissa sp.* (Kuroda 2002), which exhibits strong cytotoxicity against different human solid tumor cell lines (Lee et al. 2016). In our previous study, we reported that Jaspine B hydrochloride disrupts sphingolipid metabolism followed by elevation of Cer and induction of apoptotic cell death in HeLa cells (Bogdanova et al. 2021).

The objective of our study was to evaluate the antiproliferative effects of its epimer 2-*epi*-jaspine B (M1), focusing on its ability to induce apoptosis and autophagic cell death, as well as its impact on sphingolipid metabolism in a cervical cancer model.

Materials and Methods

Cell Culture

The human cancer cell line HeLa (adenocarcinoma of cervix) and non cancerous cell line CCD-Co18 (human colon fibroblasts) were obtained from American Type Culture collection (ATCC, Manassas, VA, USA). HeLa cells were cultured in growth medium RPMI 1640 (Biosera, Kansas City, MO, USA) and CCD-Co18 in Dulbecco's modified Eagle's Medium (DMEM). Both growth media were supplemented with 10% fetal bovine serum (FBS; Gibco, Thermo Scientific, Rockford, IL, USA) antibiotic/antimycotic solution (Merck, Darmstadt, Germany). Cells were maintained in standard conditions with an atmosphere containing 5% CO_2 in humidified air at 37°C. Cell viability, estimated by trypan exclusion, was greater than 95% before each experiment.

Tested compound

2-*epi*-jaspine hydrochloride ((2R,3S,4S)-4-amino-2-tetradecyltetrahydrofuran-3-ol hydrochloride) was synthesized and the structure was confirmed by Mass spectrometry and ^{1}H, ^{13}C NMR, and IR spectroscopy at the Department of Chemistry, Faculty of Science, Pavol Jozef Šafarik University in Košice (Mezeiova et al. 2016). The tested compound was dissolved in dimethyl sulfoxide (DMSO; Sigma-Aldrich, St. Louis, Missouri, USA). The final concentration of DMSO in cultured medium was 0.02% and exhibited no cytotoxicity on cells in each experiment.

Cell viability assay (MTS test)

To determinate half maximal-inhibitory concentration (IC_{50}) and verify an antiproliferative effect of M1, MTS colorimetric assay ((3-(4,5-dimethylthiazol-2-yl)-5-(3-carboxymethoxyphenyl)-2-(4-sulfophenyl)-2H-tetrazolium) was used. HeLa cells (5×10^3/well) were seeded in 96-well polystyrene microplates (SARSTEDT, Nümbrecht, Germany) and treated with M1 (1–10 µmol/l) for 72 h. After incubation, 10 µl of MTS reagent (5 mg/ml; Sigma Aldrich, St.Louis, MO, USA) was added, and absorbance at 490 nm was measured after 3 h using a Cytation™ Multi-Mode Reader (BioTek, USA). The absorbance of control cells was taken as 100% and the results were expressed as a percentage of control.

Scratch assay

To evaluate cell migration, confluent HeLa monolayers were cultured in 6-well plates and a uniform scratch was made across the cell monolayers using the SPL Scar™ Scratcher (SPL Life Sciences, Pocheon, Republic of Korea). After washing with PBS, cells were treated with compound M1 at various concentrations (ranging from IC_{10} to IC_{50}) in fresh medium. Cells were subsequently stained with Hoechst 33342 (Sigma-Aldrich, St. Louis, MO, USA) at 0, 24, 48 and 72 h after treatment and images of the wound area were captured using a Cytation™ 3 Cell Imaging Multi-Mode Reader (BioTek, Winooski, VT, USA). Migration distance (gap size) and wound closure were analyzed using Gen5 software (BioTek, Winooski, VT, USA).

Western blot analysis

HeLa cells were treated with compound M1 (6.5 µmol/l) for 24, 48 and 72 h. Cells were scraped, washed with PBS, and lysed in cold Laemmli buffer containing protease and phosphatase inhibitors, followed by sonication. Protein concentrations were measured using the Pierce® BCA Protein Assay Kit (Thermo Scientific, Rockford, IL, USA) and measured using an automed Cytation™ 3 Cell Imaging Multi-Mode Reader (Biotek, Winooski, VT, IL, USA) at wavelength 570 nm. Equal protein amounts (30–40 µg) were separated on 10% SDS-PAGE gels and transferred to PVDF membranes using the iBlot™ 2 system (Thermo Scientific, Rockford, IL, USA). Membranes were blocked with 5% non-fat milk (Cell Signalling Technology©, Danvers, MA, USA) or bovine serum albumine (SERVA, Heidelberg, Germany) in TBS-Tween and incubated overnight at 4°C with primary antibodies (Table 1). After washing, membranes were incubated with with corresponding HRP-conjugated secondary antibodies for 1 hour at RT (Table 1). Protein expression was visualized using chemiluminescent ECL substrate (Thermo Scientific, Rockford, IL, USA) and detected with the MF-ChemiBIS 2.0 Imag-

Table 1. List of antibodies used in Western blot analysis

Primary antibody	Mr (kDa)	Origin	Dilution	Catalouge No.	Manufacturer
Bad (D24A9)	23	Rabbit	1:1000	#9239	Cell Signalling Technology, Danvers, MA, USA
Phospho-Bad (Ser136) Antibody	23	Rabbit	1:1000	#9295	
Bax (D2E11) Rabbit mAb	20	Rabbit	1:1000	#5023	
Phospo-Bcl-2 (Ser70) (5H2) Rabbit mAb	28	Rabbit	1:1000	#2827	
Bim (C34C5) Rabbit mAb	12/15/23	Rabbit	1:1000	#2933	
Cleaved Caspase 8 (Asp374) (18C8) Rabbit mAb	43/41/18	Rabbit	1:1000	#9496	
PARP (46D11) Rabbit mAb	116/89	Rabbit	1:1000	#9532	
Beclin-1 (D40C5)	60	Rabbit	1:1000	#3495	
Phospho-ULK1 (Ser757) (D706U)	140–150	Rabbit	1:1000	#14202	
ATG7 (D12B11) RAbbit mAb	78	Rabbit	1:1000	#8558	
LC3A/B (D3U4C) XP® Rabbit mAb	14/16	Rabbit	1:1000	#12741	
LAMP1 (D2D11) XP® Rabbit mAb	90–120	Rabbit	1:1000	#9091	
ß-actin (8H10D10) Mouse mAb	45	Mouse	1:1000	#3700	
Anti-Acid sphingomyelinase antibody	65–70	Mouse	1:1000	Ab74281	Abcam
Anti-Bcl2 Antibody [100/D5]	26	Mouse	1:500	Ab692	
Bid Recombinant Rabbit mAb (JM11-14)	22	Rabbit	1:1000	MA5-32642	ThermoFisher Scientific
Secondary antibody					
Anti-Rabbit IgG HRP-Linked Antibody	–	Goat	1:1000	#7074	Cell Signaling Technology, Danvers, MA, USA
Anti-Mouse IgG HRP-Linked Antibody	–	Goat	1:1000	#7076	

ing System (DNR Bio-Imaging Systems, Jerusalem, Israel) and IBright™ FL1500 Imaging System (Thermo Fisher Scientific, Cleveland, OH, USA). Densitometry was performed using iBright Analysis software (Thermo Fisher Scientific, Cleveland, OH, USA) and Image Studio Lite Software (Thermo Fisher Scientific, Cleveland, OH, USA) and ß-actin was used as a loading control.

Flow cytometric analysis

Cell proliferation analysis

To analyse the proliferation of HeLa cells, a 5 mM stock of Cell Trace ™ Yellow Cell Proliferation Kit for flow cytometry was used (Thermo Scientific, Rockford, IL, USA). Cells were harvested, centrifuged and the pellet was resuspended in 1 ml of staining solution (2 ml Cell Trace ™ in 1 ml of PBS). Cells were incubated for 30 min at RT in the dark. After incubation, cells were resuspended in a culture medium and centrifuged to remove the supernatant. The pellet was resuspended in fresh culture medium and seeded in the middle Petri dishes. Cells were treated with M1 (6.5 mmol/l) and analyzed in three different times (24 h, 48 h, 72 h) and control cells also at 0 h. For analysis of stained cells, a BD FASCalibur flow cytometer (BD Biosciences, San Jose, CA, USA) was used.

Cell cycle analysis

Adherent and floating HeLa cells were harvested in different times (24 h, 48 h, 72 h) after treatment with M1 (6.5 mmol/l). Cells were washed in cold PBS and fixed in cold 70% ethanol (1 ml/sample) until analysis. The samples were store at −20°C for at least 24 h. Before analysis, cells were washed in PBS and the pellet was resuspended in a staining solution to incubate for 30 min at RT in the dark. Staining solution was composed of 0.5 mg/ml ribonuclease A, 0.2% final concentration, Triton X-100, propidium iodide 0.025 mg/ml in 500 ml PBS (all from Sigma Aldrich, St. Louis, MO, USA). Samples (minimum of 1×10^4 events) were analyzed with BD FASCalibur flow cytometer (BD Biosciences, San Jose, CA, USA) using FL-2 (585/42). Cell cycle distribution was determined by deconvolution of DNA content histograms, after discrimination of doublets (FL-2-W *vs.* FL-2-A) and other cellular aggregates, using the Dean-Jett-Fox Model plots.

Analysis of apoptosis via externalized phosphatidylserine

After seeding, cells were incubated with the tested compound M1 at a final concentration of 6.5 mmol/l. Cells were harvested after 24, 48 and 72 h of treatment, and pellet was resuspended in PBS. Cells were incubated with staining solution containing Annexin V-Alexa Fluor ® 647 (1:300, Thermo Scientific, Rockford, IL, USA) for 30 min at RT in the dark. Subsequently, PI (Sigma-Aldrich, Steinheim, Germany) was added to each sample at a final concentration of 25 mg/ml. The FL-2 (585/42) *vs.* FL-4 (661/16) were used to analyze the data in FlowJo software v.10 (BD Biosciences, San Jose, CA, USA).

Detection of mitochondrial membrane potential

HeLa cells were seeded at middle Petri dishes and treated with M1 (6.5 mmol/l) for 24, 48 and 72 h. Floating and adherent cells were harvested, washed in PBS and transferred to cytometric tubes for analysis. Cells were stained with TMRE (tetramethylrhodamine ethyl ester percholate; Molecular Probes, Eugene, OR, USA) at a final concentration 0.1 mmol/l. Fluorescence was detected after 30 min incubation at RT in the dark using the FL-2 (585/42) channel to collect the fluorescence signal. The data were analyzed by the FlowJo software (BD Biosciences, San Jose, CA, USA).

Fluorescent analysis of activated caspase 3/7

For this purpose, Cell Event™ Caspase 3/7 Green flow cytometry assay kit was used. Cells were harvested and pelleted at different times (24 h, 48 h, 72 h). Pellets were resuspended in 1 ml of PBS and transferred to flow cytometric tubes. 1 ml of CellEvent™ Caspase 3/7 Green Detection Reagent was added to each sample and mixed gently. Samples were incubated for 30 min at RT in the dark. In the final 5 min of staining, 1 ml of 1 mM SYTOX™ AADvanced™ dead cell stain was added to each cytometric tube.The FL-1 (530/30) *vs.* FL-4 (661/16) were used to collect the fluorescence signals and data were analyzed using FlowJo software v.10 (BD Biosciences, San Jose, CA, USA).

Flow cytometry analysis of apoptosis, autophagy and ceramide associated proteins

To perform these analyses, HeLa cells were seeded in middle Petri dishes and were treated with M1 (6,5 mmol/l). Floating and adherent cells were harvested after 24, 48 and 72 h incubation with M1 and washed in PBS. Cells were transferred into flow cytometric tubes and fixed with 4% p-formaldehyd for 20 min. For permeabilization of cells, 96% methanol was added to each sample and incubated for 15 min. After centrifugation cells were stained with conjugated antibody or with primary antibody (Table 2) and incubated for 30 min at RT in the dark, followed by staining with secondary antibody (Table 2) if needed. The antibodies and their dilutions are listed in Table 2. The data were analyzed with the

Table 2. List of antibodies used in flow cytometric analyses

Primary antibody	Dilution	Catalouge No.	Manufacturer
Cytochrome c Antibody (6H2) FITC Conjugate	1:300	11-6601-08	ThermoFisher Scientific
Anti-SQSTM1/p62 antibody (Alexa Fluor 488 antibody)	1:500	ab185015	Abcam, Cambridge, UK
Anti-ceramide Mouse IgM mAb (BSA conjugate)	1:200	ab206461	
Secondary antibody			
Alexa FluorTM 488 goat anti-rabbit IgG	1:300	A-11008	ThermoScientific Rockford, IL, USA
Alexa FluorTM 488 goat anti-mouse	1:300	A28175	

FlowJo software v.10 (BD Biosciences, San Jose, CA, USA). In software analyses the measured cell population density plot was cleaned of debris and disintegrated cells through SSC (side scatter, granularity) *vs.* FCS (forward scatter, size) properties. Following gating was performed based on fluorescence detection in FL channels to distinquish positive or negative populations in particular analyses. Percentage of cells with positive autofluorescence (AF) signal was set as background and final positive population was calculated after AF subtraction.

RNA isolation and RT-PCR

The total cellular RNA was isolated using Qiagen RNeasy® Mini Kit (Catalog #74104) according to the manufacturer's instructions. Concentration of RNA was determined spectrophotometrically using an Implen nanophotometer (Implen, Munich, Germany) and only pure samples (A260/A230 ratio > 1,8, A260/A280 ratio = 1.8–2.0) was stored at −80°C until analysis. The RevertAid™ h Minus First Strand cDNA synthesis kit (Fermentas GmbH, St. Leon-Rot, Germany) was used for reverse transcription of tRNA (0.5 ng) into cDNA, which was then used for quantitative RT-PCR analysis on an ABI 7500 FAST Real-Time PCR System (Applied Biosystems, Foster City, CA, USA) using a Luna® Universal qPCR Master Mix (BioLabs, New England Biolabs, Ipswich, MA, USA). The primer sequences are listed in Table 3 and were obtained from the RTPrimerDB database (Lefever et al. 2009). The cycling parameters for the analysis were: 10 min of initial denaturation at 95°C followed by 40 cycles of denaturation at 95°C for 15 s, primer annealing at 60°C for 30 s and extension at 72°C for 30 s. The data were analyzed using the comparative threshold (Ct) method and normalized to GAPDH (reference gene). Melting curves were generated for each PCR reaction to verify the specificity and purity of the amplified product.

Neutral sphingomyelinase activity assay (nSMase)

Protein lysates were prepared using Laemmli lysis buffer, and concentration was determined with the Pierce BCA Protein Assay Kit (Thermo Scientific, Rockford, IL, USA). Neutral sphingomyelinase activity was measured using the Sphingomyelinase Assay Colorimetric Kit (Abcam, Cambridge, UK) on an automated Cytation™ 3 Cell Imaging Multi-Mode Reader (BioTek, Winooski, VT, USA). All

Table 3. Primers sequences used in real-time PCR analysis (Sigma-Aldrich Chemie, Steinheim, Germany)

Gene	Forward primer	Reverse primer
GADPH	5'-TGCACCACCAACTGCTTAGC-3'	5'-GGCATGGACTGTGGTCATGAG-3'
APAF-1	5'-TCCATGTATGGTGACCCATCC -3'	5'-AAGGTGGAGTACCACAGAGG-3'
BCL-XL	5′-TTACCTGAATGACCACCTA-3′	5′-ATTTCCGACTGAAGAGTGA-3′
CASP 3	5′-TGGTTCATCCAGTCGCTTTG-3′	5′-CATTCTGTTGCCACCTTTCG-3′
CASP 7	5′-AGTGACAGGTATGGGCGTTCG-3′	5′-GCATCTATCCCCCCTAAAGTGG-3′
CASP 8	5′-AGAGTCTGTGCCCAAATCAAC-3′	5′-GCTGCTTCTCTCTTTGCTGAA-3
TNF-α	5'-GGCGTGGAGCTGAGAGATAAC-3'	5'-GGTGTGGGTGAGGAGCACAT-3'
CERS2	5′-TGCCAAGATGTTTAACTACGC -3′	5′-TAGCCAAAGAAGGCAGGGTA-3′
CERS4	5'-GCTGTGGACCTTCAGAAACTG-3'	5'-GGTGCGATGCTCTCTTCATC-3'
SPHK1	5'-GATGCATGAGGTGGTGAATG-3'	5'-AACAGCAGTGTGCAGTTGAT-3'
SPHK2	5'-GAAGGCATTGTCACTGTGTC -3'	5'-GCAGAGAAGAAGCGAGCAGT-3'
S1P1	5'-GGATCGCGCGGTGTAGAC-3'	5'-GCTAGAGGGCGAGGTTGAG-3'
S1P2	5'-CACTATGTGCTCTGCGTGGT-3'	5'-GGCGATGTAGGCATATGCA-3'
S1P3	5'-CCTCATCACCACCATCCTCT-3'	5'-TGGAGTAGAGGGGCAAGATG-3'

measurements were performed according to the manufacturer's instructions.

Statistical analysis

Data are presented as mean ± standard deviation (SD). Statistical differences in screening assays were assessed using one-way ANOVA, followed by Bonferroni *post hoc* test. Other experimental data were analyzed using Student's *t*-test. For the statistical analysis, * $p < 0.05$, ** $p < 0.01$, *** $p < 0.001$ *vs.* untreated control.

Results

Cell viability, proliferation and migration activity

To evaluate the effect of M1 on HeLa cell proliferation, a colorimetric MTS assay and flow cytometric analysis using Cell TraceÔ proliferation Kit were performed. MTS assay demonstrated a significant, concentration-dependent decrease in cell viability after 72 h of treatment (Fig. 1A) with IC_{50} value for M1 was 5.6 ± 0.32 µmol/l. Furthermore, MTS test was also used to evaluate the effect of sphingoid base on cell viability of non-cancerous cell line CCD-18Co and IC_{50} value was determined to be 15.30 ± 1.2 µmol/l, with a calculated selectivity index of 2.78. Flow cytometric analysis revealed that M1 (6.5 µmol/l) significantly suppressed HeLa cell proliferation compared to control group (Fig.1B), with the most pronounced reduction observed at 72 h (Fig. 1C). Based on these findings, a working concentration of 6.5 µmol/l was selected for further experiments.

A scratch assay was performed to evaluate the effect of M1 on HeLa cell migration. As shown in Figure 2, control cells progressively repopulated the wounded area in a time-dependent manner. M1-treated cells exhibited a reduced ability to close the wound and decreased cell density, especially at higher concentrations, in comparison to untreated controls. The most pronounced effect was observed at 72 h post-treatment. Our findings indicate that the sphingoid base M1 impairs the migration and wound-healing ability of cervical cancer cells, even at non-toxic concentrations (Fig. 2).

Cell cycle progression and detection of apoptosis

Analysis of cell cycle progression revealed that treatment of HeLa cells with M1 (6.5 µmol/l) led to an accumulation of reduced DNA content in sub-G0 region indicating a pro-apoptotic effect of M1 with the most pronounced peak observed at 72 h. Moreover, a concomitant decrease in the G1 population was noted (Fig. 3A). The pro-apoptotic effect of M1 was further confirmed by Annexin V staining, which detects phosphatidylserine externalization – a hallmark of early apoptosis. In later stages, loss of membrane integrity allows propidium iodide (PI) uptake. M1 caused a significant increase in the proportion of HeLa cells in early apoptosis (Annexin V^+/PI^-) after 24 h of incubation, with this effect persisting up to 72 h. Additionally, a substantial increase in late apoptotic (Annexin V^+/PI^+) /necrotic cells (Annexin V^-/PI^+) was observed at 48 and 72 h (Fig. 3B). These findings suggest that apoptosis plays a key role in the antiproliferative effects of M1.

Activation of intrinsic mitochondrial pathway

Mitochondria play a key role in both – cell survival and apoptosis. Early in apoptosis, mitochondria lose transmembrane potential ($\Delta\Psi_m$), a marker of mitochondrial dysfunction. This can be measured using TMRE dye, which binds to active, negatively charged mitochondria. In our experiments, the sphingoid base M1 significantly increased the number

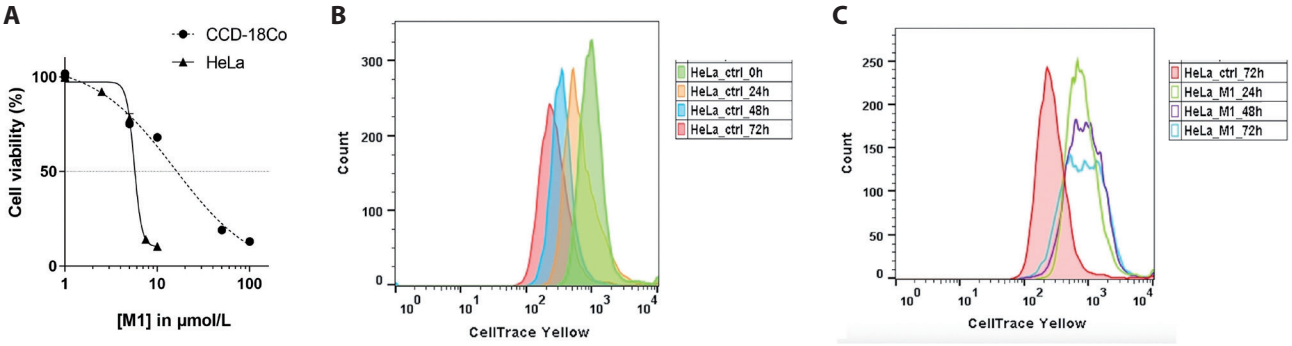


Figure 1. Effect of tested compound M1 on HeLa proliferation using a metabolic colorimetric MTS assay **A.** Flow cytometric analysis of proliferation of HeLa cells using a CellTraceÔ proliferation kit – control groups at 0, 24, 48 and 72 h (**B**) and treated HeLa cells after 24–72 h incubation with M1 compared to untreated HeLa cells at 72 h (**C**). Data are obtained from three independent experiments. ** $p < 0.01$, *** $p < 0.001$ *vs.* untreated cells (control).

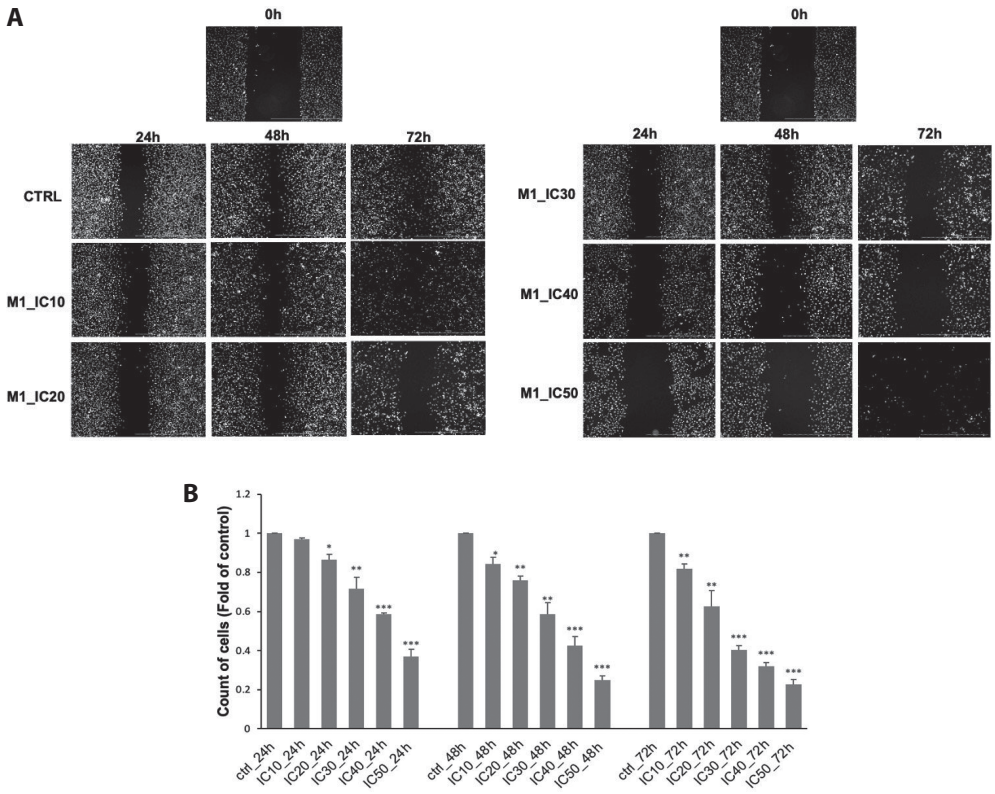


Figure 2. A. Schratch assay was performed on HeLa cells treated with IC_{10}–IC_{50} doses of M1 compared with untreated groups at 24, 48 and 72 h. **B.** Graph represents cell count in each pictures of part A. Data obtained from three independent experiments. * $p < 0.05$, ** $p < 0.01$, *** $p < 0.001$ *vs.* untreated cells (control) based on Student *t*-test.

of cells with disrupted MMP at all time points (Fig. 4A), indicating mitochondrial involvement in cell death. The Bcl-2 protein family regulates outer mitochondrial membrane permeabilization and apoptosis. As shown in Figure 5A, both pro- and antiapoptotic members show notable changes. Western blot analysis revealed a time-dependent increase in proapoptotic proteins Bax (Fig. 6G), Bid (Fig. 6E), Bim (Fig. 6F), and total Bad (Fig. 6C) along with a concurrent decrease in the phosporylated -antiapoptotic form of Bad (pBad; Fig. 6D). Reduced levels were also observed for Bcl-2 (Fig. 6B) and its antiapoptotic variant pBcl-2 (Fig. 6A). Gene expression analysis using RT-PCR showed a significant overexpression of proapoptotic *Bax* and downregulation of antiapoptotic *Bcl-XL* (Table 4). Cytochrome c, a key proapoptotic protein in the mitochondrial intermembrane space, is released when MMP dissipates and the outer membrane is damaged, triggering apoptosome formation. Our results showed significant cytochrome c release (Fig. 4B), indicating that M1 induces its release as part of apoptosis. RT-PCR also revealed overexpression of *APAF-1* (Table 4), which, together with cytochrome c and procaspase-9, forms the apoptosome – a multiprotein complex that activates caspase-9 and initi-

Table 4. Gene expression of proteins involved in apoptosis and the ceramide pathway in HeLa cells after treatment with the sphingoid base M1

Gene	24 h	48 h	72 h
	Apoptosis		
APAF1	2.722**	7. 909***	8.39***
BCL-xL	0.55**	0.207***	0.401**
BAX	1.897*	2.436**	10.419***
CASP3	1.504*	1.472*	3.209**
CASP7	1.155	1.655*	5.236***
CASP8	2.15**	1.69*	3.181**
TNF-α	1.977*	3.629**	7.997***
	Ceramide pathway		
CERS2	0.653*	1.474*	2.974**
CERS4	0.653*	2.293**	4.017***
SPHK1	0.817*	0.216***	0.69**
SPHK2	0.842*	0.341**	0.751*
S1P1	0.989	0.882*	0.774*
S1P2	0.333***	0.25***	0.317***
S1P3	1.049	1.302*	3.072**

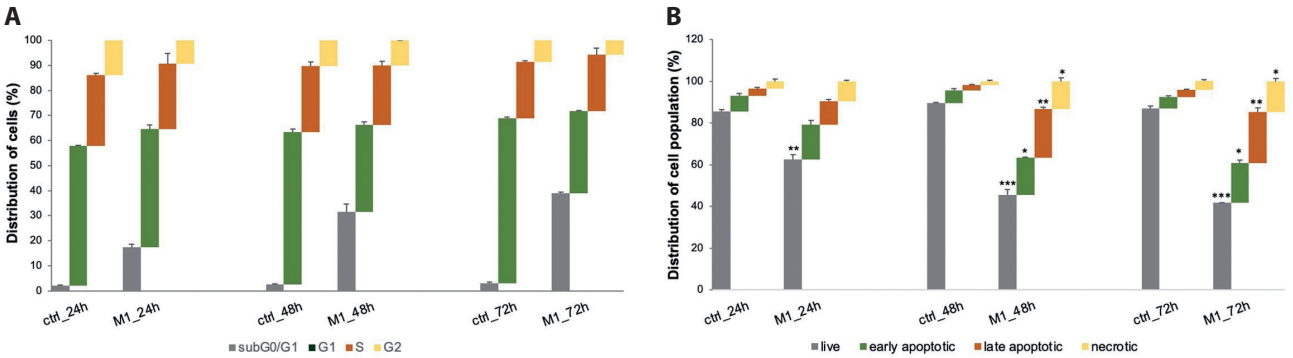


Figure 3. A. Cell cycle distribution of HeLa after 24–72 h of treatment with M1. **B.** Annexin V/PI analysis of apoptosis incidence in M1 treated HeLa cells. Data obtained from three independent experiments are presented as the mean ± SD. * $p < 0.05$, ** $p < 0.01$, *** $p < 0.001$ *vs.* untreated cells (control) based on Student *t*-test.

ates the caspase cascade. M1 treatment in HeLa cells induced cleavage of downstream effectors, procaspase-3 and -7, into their active forms. Caspase-3/7 activity peaked at 24 h, while the number of dead and necrotic cells increased progressively, reaching a maximum at 72 h post-treatment (Fig. 4C). RT-PCR analysis showed overexpression of caspase-3 and -7, with the most pronounced effect observed after 72 h of M1 exposure (Table 4). Poly(ADP-ribose) polymerase-1 (PARP-1), a well-characterized substrate of caspases, plays a critical role in DNA repair and cell survival. The presence of cleaved PARP-1 is widely recognized as a hallmark of apoptosis. Western blot analysis demonstrated that M1 treatment led to a progressive increase in cleaved PARP-1, which peaked at 72 h (Fig. 5A, Fig. 6I). We also detected additional PARP fragments (data not shown), which are presumed to arise from an alternative proteolytic mechanism distinct from the classical caspase-mediated pathway.

Activation of extrinsic pathway

The extrinsic apoptotic pathway is activated by TNF-α binding to death receptors, triggering caspase-8 activa-

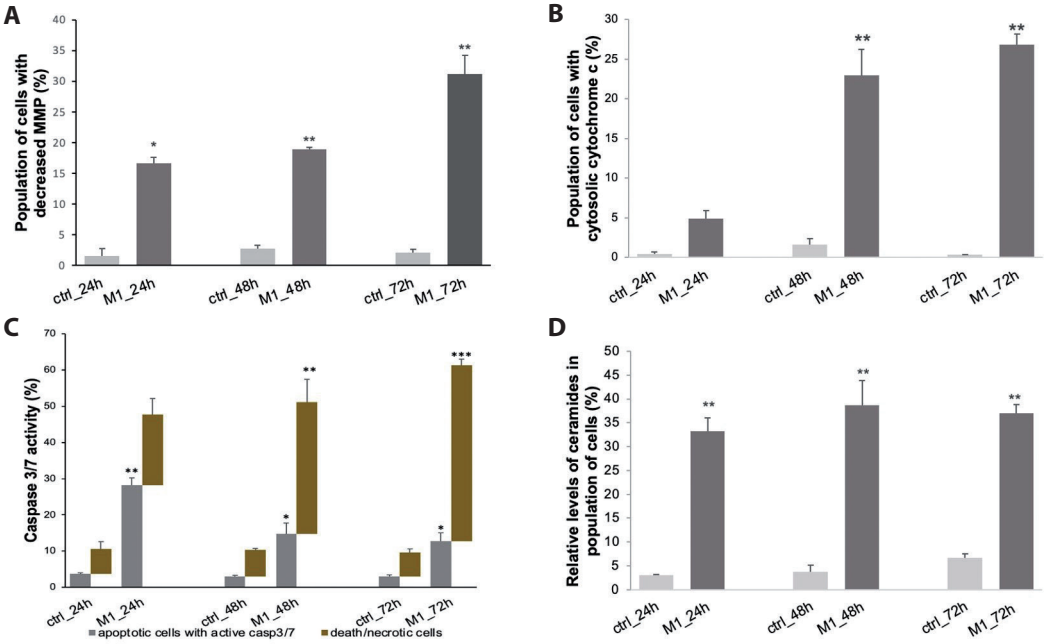


Figure 4. Flow cytometric analysis of MMP changes (**A**), cytochrome c release (**B**), activity of caspase 3/7 (**C**) and relative level of ceramides (**D**) 24, 48 and 72 h after treatment with M1 . Data represent the mean ± SD of three independent experiments. * $p < 0.05$, ** $p < 0.01$ *vs.* untreated cells (control) based on Student *t*-test.

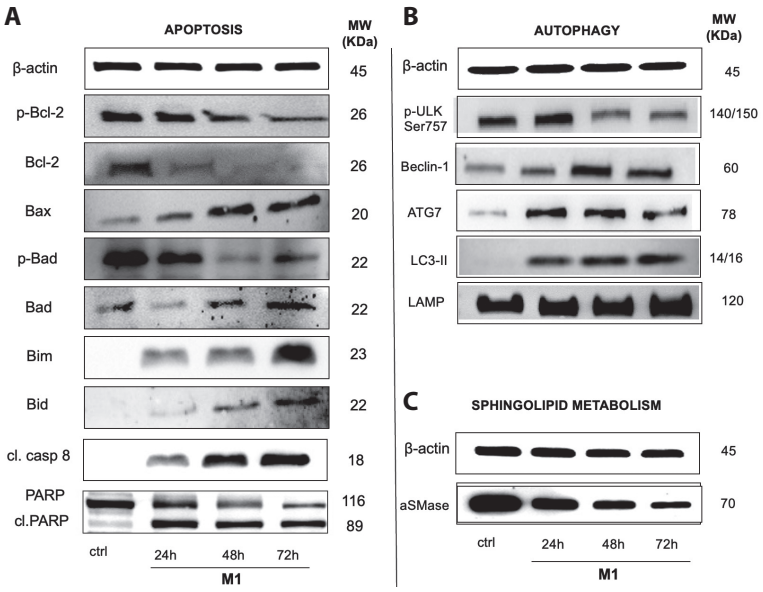


Figure 5. Western blot analysis of apoptosis related proteins (**A**), autophagy related proteins (**B**) and aSMase (**C**) in HeLa cells after treatment with M1 for 24, 48 and 72 h. Representative figures of independent experiments based on Student *t*-test.

tion initiating caspase cascade. M1 treatment significantly increased TNF-α and caspase-8 gene expression (Table 4), along with elevated levels of cleaved caspase-8 (Fig. 5A, Fig. 6H) in HeLa cells. These effects were time-dependent, peaking at 72 h, indicating that M1 induces apoptosis *via* the extrinsic pathway.

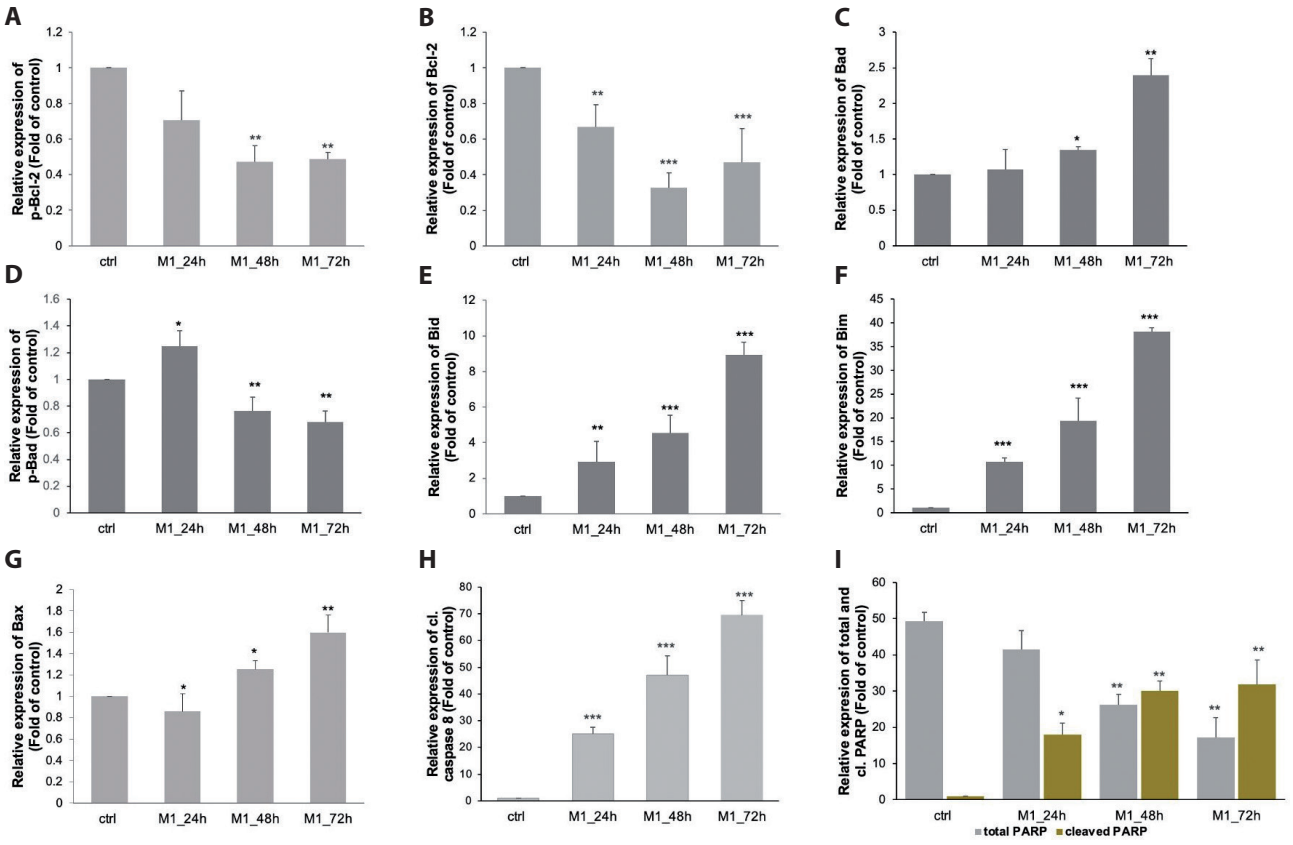


Figure 6. Densitometric analysis of Western blot assay: relative expression of p-Bcl-2 (**A**), Bcl-2 (**B**), Bad (**C**), p-Bad (**D**), Bid (**E**), Bim (**F**), Bax (**G**), caspase 8 (**H**) and PARP (**I**). * $p < 0.05$, ** $p < 0.01$, *** $p < 0.001$ *vs.* untreated cells (control) based on Student *t*-test.

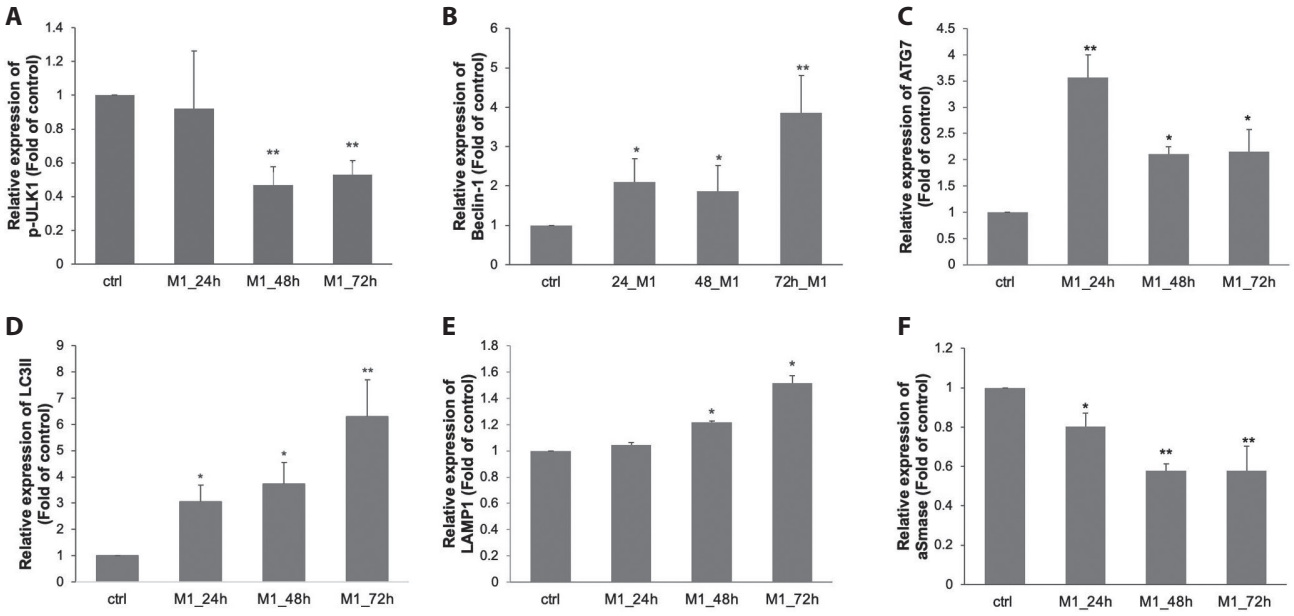


Figure 7. Densitometric analysis of autophagy related proteins and proteins involved in sphingolipid metabolism. Relative expression of p-ULK1 (**A**), Beclin-1 (**B**), ATG7 (**C**), LC3II (**D**), LAMP (**E**), aSMase (**F**). * $p < 0.05$, ** $p < 0.01$, *** $p < 0.001$ *vs.* untreated cells (control) based on Student *t*-test.

Changes in ceramide levels and sphingolipid metabolism

Ceramide (Cer), a key sphingolipid metabolite, exerts antiproliferative and pro-apoptotic effects, induces autophagy, and regulates the interplay between apoptosis and autophagy. Its balance with S1P, termed the "ceramide/S1P rheostat," is crucial for determining cell fate, with S1P promoting survival and antagonizing ceramide-induced apoptosis. Cer accumulation contributes to cell death. Flow cytometry revealed a significant increase in Cer levels in M1 treated HeLa cells as early as 24 h post-treatment, with sustained, moderate increases at 48 and 72 h (Fig. 4D). Ceramide generation under stress is mediated by SMases, particularly neutral SMase (nSMase) and acid SMase (aSMase). Colorimetric assays showed a time-dependent increase in nSMase activity, peaking at 72 h following M1 treatment (Fig. 9). In contrast, aSMase activity significantly decreased over the same period (Fig. 5C and 7F). Gene expression analysis of ceramide metabolism-related genes revealed overexpression of both *CERS2* and *4* as well as *S1P3* and downregulation of *SPHK1, 2* and *S1P1, 2* (Table 4).

Autophagic cell death

To investigate the involvement of a caspase-independent cell death mechanism, cervical carcinoma cells were treated with the sphingoid base M1 in combination with Z-VAD-fmk (zVAD), a cell-permeable, irreversible caspase inhibitor known to promote cell survival. Treatment of HeLa cells with zVAD alone increased cell viability to levels comparable to untreated controls. However, co-treatment with M1 and zVAD resulted in a significant reduction in cell viability, similar to that observed with M1 alone (Fig. 8A). These findings suggest that the antiproliferative effect of M1 may involve a caspase-independent form of cell death, such as autophagy.

ULK1 plays a key role in initiating autophagy by phosphorylating downstream targets involved in autophagosome formation. Its activity is negatively regulated by mTOR, which inhibits ULK1 through phosphorylation. Western blot analysis revealed that treatment with the sphingoid base M1 significantly reduced ULK-1 phosphorylation (Fig. 5B and 7A), suggesting that M1 may promote autophagy. Beclin 1 (Atg6; BECN1) is one of the most important autophagy-related proteins, involved in the early stage of autophagosome formation, specifically nucleation. It interacts with the Bcl-2 (Bcl-xL) protein, which acts as a negative regulator and thus as an inhibitor of autophagy. In our study, we observed significantly increased levels of BECN1 with a peak at 72 h (Fig. 5B, Fig. 7B). The subsequent expansion and closure of the phagophore membrane require lipidation of LC3 to its active form, LC3-II. LAMP1, a transmembrane glycoprotein and a major components of the lysosomal membrane, plays an importnat role in the fusion of autophagosomes with lysosomes. Western blot analysis showed a significant increase in LC3-II (Fig. 7D), ATG-7 (Fig. 7C) and LAMP1 (Fig. 7E)

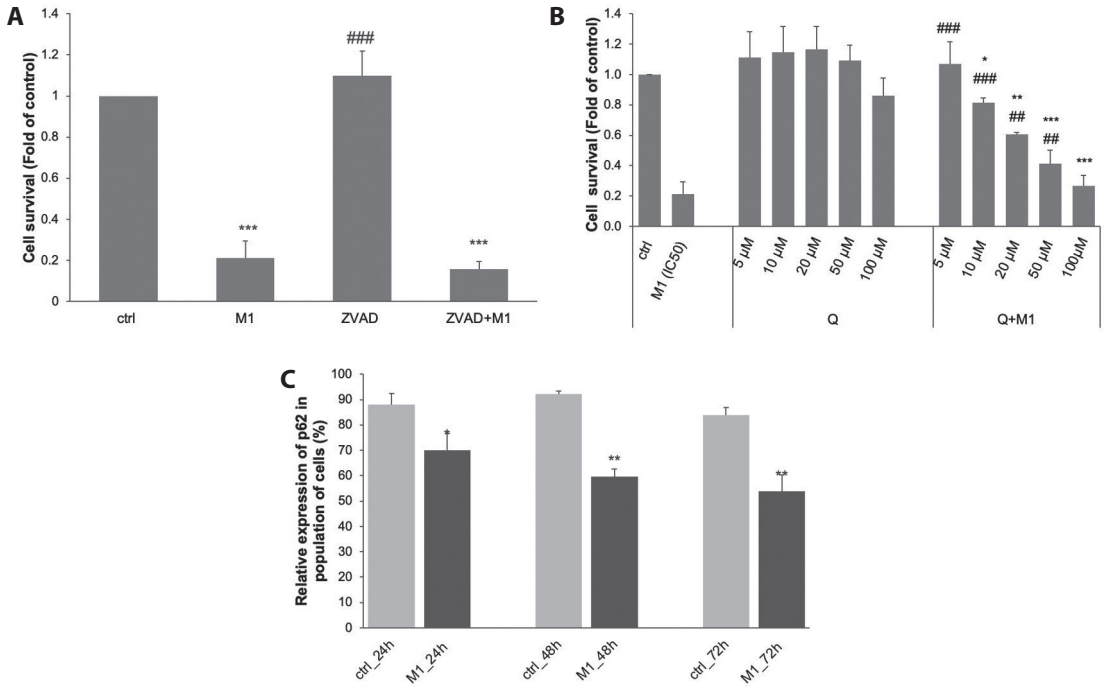


Figure 8. A. Effect of zVAD and M1 on viability of HeLa cells after 72 h incubation with M1. **B.** Effect of M1 and chloroquine on the proliferation of HeLa cells after 72 h of treatment with M1. **C.** Changes in p62 level in different analyzed times (24, 48 and 72 h) after treatmemt of HeLa cells with M1. The values show mean ± SD of three independent experiments. , * $p < 0.05$, ** $p < 0.01$, *** $p < 0.001$ *vs* .untreated cells (A,C); * $p < 0.05$, ** $p < 0.01$, *** $p < 0.001$ *vs.* chlorochin; $^{\#\#}$ $p < 0.01$, $^{\#\#\#}$ $p < 0.001$ *vs.* M1 (B) based on Student *t*-test.

protein levels in HeLa cells treated with the sphingoid base M1 (Fig. 5B). Additionally, p62 functions both as a substrate and an effector protein in autophagy. It can directly bind LC3 to facilitate cargo degradation, but its accumulation may inhibit lysosomal degradation. In our experiments, M1 treatment led to a significant decrease in p62 levels, indicating enhanced autophagic flux in cervical carcinoma cells (Fig. 8C).

To determine whether M1-induced autophagy exerts a protective effect or contributes to autophagic cell death in cervical carcinoma cells, we treated cells with a combination of the sphingoid base M1 and chloroquine (CQ), a pharmacological inhibitor of autophagy. CQ inhibits autophagic flux by preventing the formation of autolysosomes and the degradation of their contents through lysosomal pH elevation. MTS assay results showed that CQ, at non-toxic concentrations, significantly increased cell viability when combined with M1 compared to treatment with M1 alone (Fig. 8B).

Discussion

Cancer continues to be the second most common cause of death globally, posing a major challenge to public health systems (Siegel et al. 2024). Therefore, there is an urgent need to develop more potent anticancer therapeutic agents (Naeem et al. 2022). Programmed cell death (PCD), including apoptosis and autophagy, plays a central role in determining cancer cell fate. Understanding the distinct functions and interplay of these pathways offers valuable insights into cancer development and may support the discovery of novel targeted therapies. The significant rise in research on programmed cell death, particularly studies focused on apoptosis and autophagy, has greatly enriched our understanding

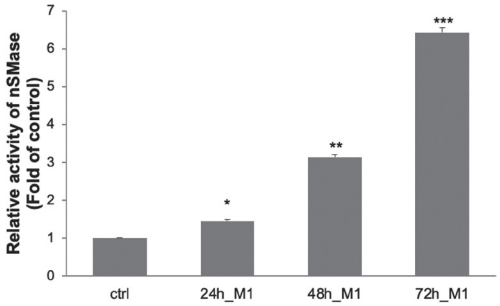


Figure 9. Colorimetric assay of activity of nSMase at different analysed times (24, 48 and 72 h) after treatment with M1. The data show mean ± SD of three independent experiments. * $p < 0.05$, ** $p < 0.01$, *** $p < 0.001$ *vs.* untreated cells (control) based on Student *t*-test.

of cancer development and treatment strategies (Ouyang et al. 2012). In this context, marine organisms have recently emerged as a promising source of novel natural compounds and synthetic drugs inspired by marine bioactive molecules (Shaik et al. 2022). Jaspine B is sponge-derived compound that exhibits antiproliferative activity against various cancer cell types, including cervical cancer cells (Bogdanova et al. 2021; Xu et al. 2022).

In our study, we focused on the antiproliferative effect of synthetic 2-*epi*-jaspine B (M1), an analog of naturally occuring anhydrosphytosphingosine, belonging to the sphingolipid family. As mentioned above, key bioactive sphingolipids participate in cell growth, differentiation, and apoptosis, thus strongly impacting tumor biology (Jia et al. 2024). In our study, treatment with the sphingoid base M1 significantly suppressed the proliferation of HeLa cells compared to untreated controls. This findings is consistent with previous studies reporting that structurally similar sphingolipids exhibit anticancer effects in various human cancer cell lines (Salma et al. 2009; Flowers et al. 2012; Sun et al. 2023). Some published data associate the antiproliferative action of sphingolipids with their ability to arrest the cell cycle in the G0/G1 or G2/M phases (Phillips et al. 2007; Kanno et al. 2014; Cai et al. 2024). Flow cytometric analysis did not reveal any such ability of M1 to induce cell cycle arrest. Instead, we observed a significant accumulation of cells in the sub-G0 phase, indicating apoptotic cell death (Abou-Hashem et al. 2019). This finding was further confirmed by Annexin V/PI staining, as the externalization of phosphatidylserine to the cell surface detectable by Annexin V is a hallmark of early-stage apoptosis (Balasubramanian et al. 2007).

Mitochondrial outer membrane permeabilization (MOMP), a key event in the intrinsic apoptotic pathway, is associated with the loss of mitochondrial membrane potential (MMP). This loss facilitates the release of cytochrome c into the cytosol, leading to the activation of caspases and proteases that mediate apoptotic cell death (Green and Kroemer 2004; Wang and Youle 2009). In our study, M1 treatment resulted in a significant increase in the number of cells exhibiting MMP loss, which was accompanied by elevated levels of cytosolic cytochrome c. We also observed increased gene expression of *APAF1*. The interaction of cytochrome c with APAF-1 activates caspase-9, which subsequently activates the effector caspases-3 and -7 (Lakhani et al. 2006). Nagahara et al. reported that the structurally similar phytosphingosine activates caspases-9, -3, and -8 in Jurkat cells. Our findings are consistent with this observation (Nagahara et al. 2005). Caspase-8 is a key mediator of extrinsic apoptosis, activated by Fas/TNF-α signaling. It triggers effector caspases or cleaves Bid to amplify mitochondrial apoptosis (Mandal et al. 2020). In our study, TNF-α and caspase-8 were upregulated, with increased cleaved caspase-8, indicating activation of the extrinsic pathway. Effector caspases promote apoptosis by cleaving key proteins like PARP-1, disabling DNA repair (Kaufmann 1993; Soldani et al. 2001; Taylor et al. 2008; Park and Chen 2012). M1 increased caspase activity and induced time-dependent PARP-1 cleavage, consistent with apoptosis triggered by sphingosine and its derivatives (Hung 1999; Chang et al. 2001; Yasui et al. 2005; Kim et al. 2009; Cai et al. 2024). MOMP and caspase activation mark the irreversible phase of apoptosis, regulated by Bcl-2 family proteins (Kulsoom et al. 2018). Our results show that M1 promotes apoptosis by reducing total/phospho-Bcl-2, increasing Bax, Bad, Bim, and cleaved Bid, and decreasing inactive phospho-Bad – activating both intrinsic and extrinsic pathways, similar to effects reported for the sphingosine analog Fingolimod (Kiyota et al. 2013).

Besides proliferation, the migratory rate is also an important factor contributing to tumor growth, metastasis formation, and drug resistance (Hamidi and Ivaska 2018). M1 treatment inhibited the migratory abibity of HeLa cells in a time- and dose-dependent manner. Additionally, we observed reduced cell proliferation at toxic concentrations, likely due to the induction of apoptosis. Similar results have been reported, where the natural sphingolipid phytosphingosine suppressed migratory potential, thereby preventing breast cancer metastasis (Kang 2017).

Because M1 structurally resembles sphingosine, we investigated its effect on sphingolipid metabolism, focusing on ceramide (Cer), a key regulator of apoptosis.

Ceramide and sphingosine levels rise in response to TNF-α, FasL, stress, and chemotherapeutic agents (Moro et al. 2019). We observed a significant Cer increase in M1-treated HeLa cells, consistent with previous studies using Jaspine B, M1's isomer, in melanoma and cervical cancer models (Bogdanova et al. 2021; Salma et al. 2009). This suggests Cer accumulation contributes to M1's antiproliferative effect. While aSMase activity decreased – possibly reflecting a biphasic Cer response – nSMase activity increased, supporting sustained Cer generation (Vit and Rosselli 2003; Shamseddine et al. 2015). These results align with findings that nSMase-derived Cer promotes mitochondrial apoptosis *via* Bax/Bcl-2 interactions (Chipuk et al. 2012). We show that M1 increases Cer levels by modulating sphingolipid metabolism. Cer accumulation is linked to upregulation of *CERS2/4* and increased nSMase activity, promoting apoptosis via the salvage pathway and SM hydrolysis. Higher expression of CERS2 has been shown to enhance chemosensitivity of breast cancer and decrease migration and invasion ability of cells (Fan et al. 2013; Fan et al. 2015). Concurrently, S1P synthesis *via* sphingosine kinases (SK1/2) reduces Cer levels and inhibits apoptosis while promoting autophagy (Spiegel and Milstien 2003; Li et al. 2014). In cervical cancer cells, SK1/2 are upregulated and linked to decreased survival (Kim et al. 2015; Xu et al.

2018). M1 downregulates SK1/2 and alters S1P receptor expression (↓*S1PR1/2*, ↑*S1PR3*), disrupting the sphingolipid rheostat and favoring cell death. Similarly, Fingolimod (a sphingosine analogue) induces non-caspase-mediated cell death *via* autophagy (Wallington-Beddoe et al. 2011) and exerts tumor-suppressive effects through inhibition of SK1 and S1P receptors (Vessey et al. 2007; Huwiler and Zangemeister-Wittke 2018). These findings highlight M1's potential to enhance anticancer responses through Cer/S1P pathway modulation.

Bioactive sphingolipids play an important role not only in apoptosis but also modulate autophagy by acting at various stages of the autophagy process (Young et al. 2013). Ceramide activates JNK, which phosphorylates Bcl-2, releasing Beclin1 to promote autophagy. In cancer cells, ceramide increases Beclin1 via JNK, enhancing autophagy (Li et al. 2009). Ceramides can also serve as autophagy substrates and affect autophagosome-lysosome fusion by modulating lipid composition (Alizadeh et al. 2023).

A key regulator of autophagy initiation is the kinase ULK-1, which plays an important role in the early stage of autophagosome formation in response to starvation or mTOR signaling. mTOR inhibits ULK-1 through phosphorylation at Ser757 (Kim et al. 2011). In our experiments, treatment of HeLa cells with the sphingoid base M1 led to a significant decrease in the phosphorylation of the ULK-1. The subsequent progression of autophagy is controlled and modulated by ATG proteins, among which Beclin1 is considered key; its levels were increased by M1 treatment. During autophagosome formation, diffuse LC3 undergoes hydrolysis followed by conjugation with phosphatidylethanolamine, mediated by ATG7 and ATG3, resulting in the lipidated form LC3-II (Frudd et al. 2018). In HeLa cells exposed to M1, increased levels of LC3-II and ATG7 proteins were observed. Since the accumulation of LC3-II-positive autophagosomes can result either from increased autophagy induction or decreased degradation, we further examined autophagic flux. p62, or sequestosome, is an autophagic receptor for LC3-II involved in substrate transport to autophagosomes and is subsequently degraded in autolysosomes. It is used as a measure of autophagic degradation efficiency (Bjørkøy et al. 2009). Upon M1 treatment, p62 levels decreased, confirming ongoing autophagy. Our results align with a study where exogenous C18-ceramide increased LC3-II levels and concurrently showed a decreasing trend in p62, leading to lethal autophagy (Wang et al. 2017). LAMP1 is the predominant lysosomal membrane protein, maintaining membrane integrity and preventing the release of lysosomal proteins into the cytoplasm (Barrachina et al. 2006). Although autophagy targets various organelles within the cell, substrates are transported to lysosomes for degradation; therefore, lysosomal dysfunction can impair autophagic flux (Pi et al. 2017). Reduced LAMP1 expression is associated with poorer patient survival (Wang et al. 2024). In cells incubated with M1, we observed increased levels of this lysosomal protein.

Conclusion

Our findings demonstrate that the sphingosine analog, 2-*epi*-jaspine B, inhibited *in vitro* proliferation of cervical cancer cells by inducing apoptosis and autophagic cell death, mediated through interference with sphingolipid metabolism and elevation of ceramide levels. Further studies are needed to clarify the mechanisms underlying the antiproliferative effects of M1. The presented data support the potential of sphingolipid derivatives as promising anticancer agents.

Conflicts of interest. The authors declare that they have no competing interests.

Acknowledgements. This research was funded by the Slovak Grant Agency for Science VEGA No 1/0278/23, VEGA No 1/0539/21. Moreover, this publication is the result of the project implementation: "Open scientific community for modern interdisciplinary research in medicine (OPENMED)", ITMS2014+: 313011V455, supported by the Operational Programme Integrated Infrastructure, funded by the ERDF. This publication is also funded by the EU NextGenerationEU through the Recovery and Resilience Plan for Slovakia under the project No. 09I03-03-V04-00751.

Data availability statement. Data are available upon request from the corresponding author.

References

Abou-Hashem MMM, Abo-Elmatty DM, Mesbah NM, Abd El-Mawgoud AM (2019): Induction of sub-G(0) arrest and apoptosis by seed extract of Moringa peregrina (Forssk.) Fiori in cervical and prostate cancer cell lines. J. Integr. Med, **17,** 410-422 https://doi.org/10.1016/j.joim.2019.09.004

Adan-Gokbulut A, Kartal-Yandim M, Iskender G, Baran Y (2013): Novel agents targeting bioactive sphingolipids for the treatment of cancer. Curr. Med. Chem. **20,** 108-122 https://doi.org/10.2174/0929867311302010011

Alizadeh J, da Silva Rosa SC, Weng X, Jacobs J, Lorzadeh S, Ravandi A, Vitorino R, Pecic S, Zivkovic A, Stark H, et al. (2023): Ceramides and ceramide synthases in cancer: Focus on apoptosis and autophagy. Eur. J. Cell. Biol. **102,** 151337 https://doi.org/10.1016/j.ejcb.2023.151337

Balasubramanian K, Mirnikjoo B, Schroit AJ (2007): Regulated externalization of phosphatidylserine at the cell surface: implications for apoptosis. J. Biol. Chem. **282,** 18357-18364 https://doi.org/10.1074/jbc.M700202200

Barrachina M, Maes T, Buesa C, Ferrer I (2006): Lysosome-associated membrane protein 1 (LAMP-1) in Alzheimer's disease. Neuropathol. Appl. Neurobiol. **32,** 505-516

https://doi.org/10.1111/j.1365-2990.2006.00756.x
Bjørkøy G, Lamark T, Pankiv S, Øvervatn A, Brech AJohansen T (2009): Monitoring Autophagic Degradation of p62/SQSTM1. Methods Enzymol. **452,** 181-197 https://doi.org/10.1016/S0076-6879(08)03612-4
Bogdanova A, Kello M, Macejova A, Nosalova N, Petik P, Takac P, Martinkova M, Mezeiova E, Mirossay L, Gal P, et al. (2021): Jaspine B hydrochloride-induced apoptosis in HeLa cells is associated with disrupted sphingolipid metabolism and ceramide overload. Anticancer Res. **41,** 2875-2883 https://doi.org/10.21873/anticanres.15069
Bray F, Laversanne M, Sung H, Ferlay J, Siegel RL, Soerjomataram I, Jemal A (2024): Global cancer statistics 2022: GLOBOCAN estimates of incidence and mortality worldwide for 36 cancers in 185 countries. CA Cancer J. Clin. **74,** 229-263 https://doi.org/10.3322/caac.21834
Cai Q, Chen M, Wang B, Wang J, Xia L, Li J (2024): Phytosphingosine inhibits the growth of lung adenocarcinoma cells by inducing G2/M-phase arrest, apoptosis, and mitochondria-dependent pathway cell death in vitro and in vivo. Chem. Biol. Interact. **387,** 110795 https://doi.org/10.1016/j.cbi.2023.110795
Fan S, Niu Y, Tan N, Wu Z, Wang Y, You H, Ke R, Song J, Shen Q, Wang W, et al. (2013): LASS2 enhances chemosensitivity of breast cancer by counteracting acidic tumor microenvironment through inhibiting activity of V-ATPase proton pump. Oncogene **32,** 1682-1690 https://doi.org/10.1038/onc.2012.183
Fan SH, Wang YY, Lu J, Zheng YL, Wu DM, Zhang ZF, Shan Q, Hu B, Li MQ, Cheng W (2015): CERS2 suppresses tumor cell invasion and is associated with decreased V-ATPase and MMP-2/MMP-9 activities in breast cancer. J. Cell Biochem. **116,** 502-513 https://doi.org/10.1002/jcb.24978
Flowers M, Fabrias G, Delgado A, Casas J, Abad JL, Cabot MC (2012): C6-ceramide and targeted inhibition of acid ceramidase induce synergistic decreases in breast cancer cell growth. Breast Cancer Res. Treat. **133,** 447-458 https://doi.org/10.1007/s10549-011-1768-8
Frudd K, Burgoyne T, Burgoyne JR (2018): Oxidation of Atg3 and Atg7 mediates inhibition of autophagy. Nat. Commun. **9,** 95 https://doi.org/10.1038/s41467-017-02352-z
Furuya H, Shimizu Y, Kawamori T (2011): Sphingolipids in cancer. Cancer Metastasis Rev. **30,** 567-576 https://doi.org/10.1007/s10555-011-9304-1
George IA, Chauhan R, Dhawale RE, Iyer R, Limaye S, Sankaranarayanan R, Venkataramanan R, Kumar P (2022): Insights into therapy resistance in cervical cancer. Advances in Cancer Biology – Metastasis. **6,** 100074 https://doi.org/10.1016/j.adcanc.2022.100074
Green DR, Kroemer G (2004): The pathophysiology of mitochondrial cell death. Science **305,** 626-629 https://doi.org/10.1126/science.1099320
Guida F, Kidman R, Ferlay J, Schuz J, Soerjomataram I, Kithaka B, Ginsburg O, Mailhot Vega RB, Galukande M, Parham G, et al. (2022): Global and regional estimates of orphans attributed to maternal cancer mortality in 2020. Nat. Med. **28,** 2563-2572 https://doi.org/10.1038/s41591-022-02109-2
Hamidi H, Ivaska J (2018): Every step of the way: integrins in cancer progression and metastasis. Nat. Rev. Cancer. **18,** 533-548 https://doi.org/10.1038/s41568-018-0038-z
Hannun YA, Obeid LM (2008): Principles of bioactive lipid signalling: lessons from sphingolipids. Nat. Rev. Mol. Cell Biol. **9,** 139-150 https://doi.org/10.1038/nrm2329
Hung W, Chang H, Chuang L (1999): Activation of caspase-3-like proteases in apoptosis induced by sphingosine and pther long-chain bases in Hep3B hepatoma cells. Biochem. J. **338,** 161-166 https://doi.org/10.1042/bj3380161
Huwiler A, Zangemeister-Wittke U (2018): The sphingosine 1-phosphate receptor modulator fingolimod as a therapeutic agent: Recent findings and new perspectives. Pharmacol. Ther. **185,** 34-49 https://doi.org/10.1016/j.pharmthera.2017.11.001
Chang HC, Tsai LH, Chuang LY, Hung WC (2001): Role of AKT kinase in sphingosine-induced apoptosis in human hepatoma cells. J. Cell Physiol. **188,** 188-193 https://doi.org/10.1002/jcp.1108
Chaudhry GE, Md Akim A, Sung YY, Sifzizul TMT (2022): Cancer and apoptosis: The apoptotic activity of plant and marine natural products and their potential as targeted cancer therapeutics. Front. Pharmacol. **13,** 842376 https://doi.org/10.3389/fphar.2022.842376
Chipuk JE, McStay GP, Bharti A, Kuwana T, Clarke CJ, Siskind LJ, Obeid LM, Green DR (2012): Sphingolipid metabolism cooperates with BAK and BAX to promote the mitochondrial pathway of apoptosis. Cell **148,** 988-1000 https://doi.org/10.1016/j.cell.2012.01.038
Jia W, Yuan J, Zhang J, Li S, Lin W, Cheng B (2024): Bioactive sphingolipids as emerging targets for signal transduction in cancer development. Biochim. Biophys. Acta Rev. Cancer **1879,** 189176 https://doi.org/10.1016/j.bbcan.2024.189176
Kang HM, Son HS, Cui YH, Youn B, Son B, Kaushik NK, Uddin N, Lee, JS, Song JY, Kaushik N, Lee, SJ (2017): Phytosphingosine exhibits an anti-epithelial-mesenchymal transition function by the inhibition of EGFR signaling in human breast cancer cells. Oncotarget **8,** 77794-77808 https://doi.org/10.18632/oncotarget.20783
Kanno T, Gotoh A, Nishizaki T (2014): Sphingosine arrests the cell cycle and induces apoptosis by targeting sphingosine-dependent protein kinase and protein kinase Cδ in vitro. Personalized Medicine Universe **3,** 22-27 https://doi.org/10.1016/j.pmu.2014.03.003
Kaufmann S, Desnoyers S, Ottaviano Y, Davidson NE, Poirier GG (1993): Specific cleavage of poly-(-ADP-ribose)-polymerase: an early marker of chemotherapy-induced apoptosis. Cancer Res. **53,** 3976-3985
Kim BM, Choi YJ, Han Y, Yun YS, Hong SH (2009): N,N-dimethyl phytosphingosine induces caspase-8-dependent cytochrome c release and apoptosis through ROS generation in human leukemia cells. Toxicol. Appl. Pharmacol. **239,** 87-97 https://doi.org/10.1016/j.taap.2009.05.020
Kim HS, Yoon G, Ryu JY, Cho YJ, Choi JJ, Lee YY, Kim TJ, Choi CH, Song SY, Kim BG, et al. (2015): Sphingosine kinase 1 is

a reliable prognostic factor and a novel therapeutic target for uterine cervical cancer. Oncotarget **6,** 26746-26756 https://doi.org/10.18632/oncotarget.4818

Kim J, Kundu M, Viollet B, Guan KL (2011): AMPK and mTOR regulate autophagy through direct phosphorylation of Ulk1. Nat. Cell Biol. **13,** 132-141 https://doi.org/10.1038/ncb2152

Kitatani K, Idkowiak-Baldys J, Hannun YA (2008): The sphingolipid salvage pathway in ceramide metabolism and signalling. Cell Signal. **20,** 1010-1018 https://doi.org/10.1016/j.cellsig.2007.12.006

Kiyota M, Kuroda J, Yamamoto-Sugitani M, Shimura Y, Nakayama R, Nagoshi H, Mizutani S, Chinen Y, Sasaki N, Sakamoto N, et al. (2013): FTY720 induces apoptosis of chronic myelogenous leukemia cells via dual activation of BIM and BID and overcomes various types of resistance to tyrosine kinase inhibitors. Apoptosis **18,** 1437-1446 https://doi.org/10.1007/s10495-013-0882-y

Knoff J, Yang B, Hung CF, Wu TC (2014): Cervical cancer: Development of targeted therapies beyond molecular pathogenesis. Curr. Obstet. Gynecol. Rep. **3,** 18-32 https://doi.org/10.1007/s13669-013-0068-1

Kulsoom B, Shamsi TS, Afsar NA, Memon Z, Ahmed N, Hasnain SN (2018): Bax, Bcl-2, and Bax/Bcl-2 as prognostic markers in acute myeloid leukemia: are we ready for Bcl-2-directed therapy?. Cancer Manag. Res. **10,** 403-416 https://doi.org/10.2147/CMAR.S154608

Kumar MS, Adki KM (2018): Marine natural products for multi-targeted cancer treatment: A future insight. Biomed. Pharmacother. **105,** 233-245 https://doi.org/10.1016/j.biopha.2018.05.142

Kuroda I, Musman M, Ohtani II, Toshio I, Tanaka J, Gravalos DG, Higa T (2002): Pachastrissamine, a cytotoxic anhydrophytosphingosine from a marine sponge, Pachastrissa sp. J. Nat. Prod. **65,** 1505-1506 https://doi.org/10.1021/np010659y

Lakhani SA, Masud A, Kuida K, Porter GA, Jr., Booth CJ, Mehal WZ, Inayat I, Flavell RA (2006): Caspases 3 and 7: key mediators of mitochondrial events of apoptosis. Science **311,** 847-851 https://doi.org/10.1126/science.1115035

Lee J, Choi K, Kwon M, Lee D, Choi MK, Song IS (2016): Differential cytotoxic effects of jaspine B in various cancer cells. J. Life Science **26,** 1392-1399 https://doi.org/10.5352/JLS.2016.26.12.1392

Lefever S, Vandesompele J, Speleman F, Pattyn F (2009): RTPrimerDB: the portal for real-time PCR primers and probes. Nucleic Acids Res. **37,** 942-945 https://doi.org/10.1093/nar/gkn777

Li DD, Wang LL, Deng R, Tang J, Shen Y, Guo JF, Wang Y, Xia LP, Feng GK, Liu QQ, et al. (2009): The pivotal role of c-Jun NH2-terminal kinase-mediated Beclin 1 expression during anticancer agents-induced autophagy in cancer cells. Oncogene **28,** 886-898 https://doi.org/10.1038/onc.2008.441

Li Y, Li S, Qin X, Hou W, Dong H, Yao L, Xiong L (2014): The pleiotropic roles of sphingolipid signaling in autophagy. Cell Death Dis. **5,** e1245 https://doi.org/10.1038/cddis.2014.215

Mandal R, Barron JC, Kostova I, Becker S, Strebhardt K (2020): Caspase-8: The double-edged sword. Biochim. Biophys. Acta Rev. Cancer. **1873,** 188357 https://doi.org/10.1016/j.bbcan.2020.188357

Mezeiova E, Martinkova M, Stankova K, Fabisikova M, Gonda J, Pilatova M, Gonciova G (2016): Total synthesis and antiproliferative/cytotoxic profiling of 2-epi-jaspine B. Carbohydr. Res. **423,** 70-81 https://doi.org/10.1016/j.carres.2016.01.011

Moro K, Nagahashi M, Gabriel E, Takabe K, Wakai T (2019): Clinical application of ceramide in cancer treatment. Breast Cancer **26,** 407-415 https://doi.org/10.1007/s12282-019-00953-8

Naeem A, Hu P, Yang M, Zhang J, Liu Y, Zhu W, Zheng Q (2022): Natural products as anticancer agents: current status and future perspectives. Molecules **27,** 8367 https://doi.org/10.3390/molecules27238367

Nagahara Y, Shinomiya T, Kuroda S, Kaneko N, Nishio R, Ikekita M (2005): Phytosphingosine induced mitochondria-involved apoptosis. Cancer Sci. **96,** 83-92 https://doi.org/10.1111/j.1349-7006.2005.00012.x

Newton J, Lima S, Maceyka M, Spiegel S (2015): Revisiting the sphingolipid rheostat: Evolving concepts in cancer therapy. Exp. Cell Res. **333,** 195-200 https://doi.org/10.1016/j.yexcr.2015.02.025

Nurgali K, Jagoe RT, Abalo R (2018): Editorial: Adverse effects of cancer chemotherapy: anything new to improve tolerance and reduce sequelae?. Front. Pharmacol. **9,** 245 https://doi.org/10.3389/fphar.2018.00245

Ogretmen B (2018): Sphingolipid metabolism in cancer signalling and therapy. Nat. Rev. Cancer **18,** 33-50 https://doi.org/10.1038/nrc.2017.96

Ogretmen B, Hannun YA (2004): Biologically active sphingolipids in cancer pathogenesis and treatment. Nat. Rev. Cancer **4,** 604-616 https://doi.org/10.1038/nrc1411

Ouyang L, Shi Z, Zhao S, Wang FT, Zhou TT, Liu BBao JK (2012): Programmed cell death pathways in cancer: a review of apoptosis, autophagy and programmed necrosis. Cell Prolif. **45,** 487-498 https://doi.org/10.1111/j.1365-2184.2012.00845.x

Park SR, Chen A (2012): Poly(adenosine diphosphate-ribose) polymerase inhibitors in cancer treatment. Hematol. Oncol. Clin. North Am. **26,** 649-670 https://doi.org/10.1016/j.hoc.2012.02.012

Phillips DC, Hunt JT, Moneypenny CG, Maclean KH, McKenzie PP, Harris LC, Houghton JA (2007): Ceramide-induced G2 arrest in rhabdomyosarcoma (RMS) cells requires p21Cip1/Waf1 induction and is prevented by MDM2 overexpression. Cell Death Differ. **14,** 1780-1791 https://doi.org/10.1038/sj.cdd.4402198

Pi H, Li M, Tian L, Yang Z, Yu Z, Zhou Z (2017): Enhancing lysosomal biogenesis and autophagic flux by activating the transcription factor EB protects against cadmium-induced neurotoxicity. Sci. Rep. **7,** 43466 https://doi.org/10.1038/srep43466

Pyne NJ, Pyne S (2010): Sphingosine 1-phosphate and cancer. Nat. Rev. Cancer **10,** 489-503

https://doi.org/10.1038/nrc2875
Salma Y, Lafont E, Therville N, Carpentier S, Bonnafe MJ, Levade T, Genisson Y, Andrieu-Abadie N (2009): The natural marine anhydrophytosphingosine, Jaspine B, induces apoptosis in melanoma cells by interfering with ceramide metabolism. Biochem. Pharmacol. **78,** 477-485
https://doi.org/10.1016/j.bcp.2009.05.002
Shaik BB, Katari NK, Jonnalagadda SB (2022): Role of natural products in developing novel anticancer agents: A perspective. Chem. Biodivers. **19,** e202200535
https://doi.org/10.1002/cbdv.202200535
Shamseddine AA, Airola MV, Hannun YA (2015): Roles and regulation of neutral sphingomyelinase-2 in cellular and pathological processes. Adv. Biol. Regul. **57,** 24-41
https://doi.org/10.1016/j.jbior.2014.10.002
Siegel RL, Giaquinto AN, Jemal A (2024): Cancer statistics 2024. CA Cancer J. Clin. **74,** 12-49
https://doi.org/10.3322/caac.21820
Soldani C, Lazze MC, Bottone MG, Tognon G, Biggiogera M, Pellicciari CE, Scovassi AI (2001): Poly(ADP-ribose) polymerase cleavage during apoptosis: when and where? Exp. Cell Res. **269,** 193-201
https://doi.org/10.1006/excr.2001.5293
Spiegel S, Milstien S (2003): Sphingosine-1-phosphate: an enigmatic signalling lipid. Nat. Rev. Mol. Cell Biol. **4,** 397-407
https://doi.org/10.1038/nrm1103
Sun C, Chang X, MacIsaac HJ, Wen J, Zhao L, Dai Z, Li J (2023): Phytosphingosine inhibits cell proliferation by damaging DNA in human cell lines. Ecotoxicol. Environ. Saf. **256,** 114840
https://doi.org/10.1016/j.ecoenv.2023.114840
Taylor RC, Cullen SP, Martin SJ (2008): Apoptosis: controlled demolition at the cellular level. Nat. Rev. Mol. Cell Biol. **9,** 231-241
https://doi.org/10.1038/nrm2312
Vessey DA, Kelley M, Zhang J, Li L, Tao R, Karliner JS (2007): Dimethylsphingosine and FTY720 inhibit the SK1 form but activate the SK2 form of sphingosine kinase from rat heart. J. Biochem. Mol. Toxicol. **21,** 273-279
https://doi.org/10.1002/jbt.20193
Vit JP, Rosselli F (2003): Role of the ceramide-signaling pathways in ionizing radiation-induced apoptosis. Oncogene **22,** 8645-8652
https://doi.org/10.1038/sj.onc.1207087
Wallington-Beddoe CT, Hewson J, Bradstock KF, Bendall LJ (2011): FTY720 produces caspase-independent cell death of acute lymphoblastic leukemia cells. Autophagy **7,** 707-715
https://doi.org/10.4161/auto.7.7.15154
Wang C, Youle RJ (2009): The role of mitochondria in apoptosis. Annu Rev. Genet. **43,** 95-118
https://doi.org/10.1146/annurev-genet-102108-134850
Wang X, Fang L, Xiao L, Zhong G, Han M, Wang B, Ren J, Zang Y (2024): Research on the effect of LAMP1 in the development and progression of ccRCC and its potential mechanism with LC3C-mediated autophagy. Front. Immunol. **15,** 1494005
https://doi.org/10.3389/fimmu.2024.1494005
Wang Z, Wen L, Zhu F, Wang Y, Xie Q, Chen Z, Li Y (2017): Overexpression of ceramide synthase 1 increases C18-ceramide and leads to lethal autophagy in human glioma. Oncotarget **8,** 104022-104036
https://doi.org/10.18632/oncotarget.21955
Xu F, Xie Q, Li YW, Jing QQ, Liu XJ, Xu YC, Wang X, Liu L, Kim G, Choi Y (2022): Suppression of JNK/ERK dependent autophagy enhances Jaspine B derivative-induced gastric cancer cell death via attenuation of p62/Keap1/Nrf2 pathways. Toxicol. Appl. Pharmacol. **438,** 115908
https://doi.org/10.1016/j.taap.2022.115908
Xu L, Jin L, Yang B, Wang L, Xia Z, Zhang Q, Xu J (2018): The sphingosine kinase 2 inhibitor ABC294640 inhibits cervical carcinoma cell growth. Oncotarget **9,** 2384-2394
https://doi.org/10.18632/oncotarget.23415
Yasui H, Hideshima T, Raje N, Roccaro AM, Shiraishi N, Kumar S, Hamasaki M, Ishitsuka K, Tai YT, Podar K, et al. (2005): FTY720 induces apoptosis in multiple myeloma cells and overcomes drug resistance. Cancer Res. **65,** 7478-7484
https://doi.org/10.1158/0008-5472.CAN-05-0850
Young MM, Kester M, Wang HG (2013): Sphingolipids: regulators of crosstalk between apoptosis and autophagy. J. Lipid Res. **54,** 5-19
https://doi.org/10.1194/jlr.R031278

Received: May 28, 2025
Final version accepted: August 14, 2025